How to cite: *Angew. Chem. Int. Ed.* **2021**, *60*, 2974–2979
International Edition: doi.org/10.1002/anie.202012504
German Edition: doi.org/10.1002/ange.202012504

Covalent Organic Frameworks | Hot Paper

Rational Construction of Borromean Linked Crystalline Organic Polymers

*Xiuxiu Guo[+], En Lin[+], Jia Gao, Tianhui Mao, Dong Yan, Peng Cheng, Shengqian Ma, Yao Chen, and Zhenjie Zhang**

Dedicated to the 100th anniversary of Chemistry at Nankai University

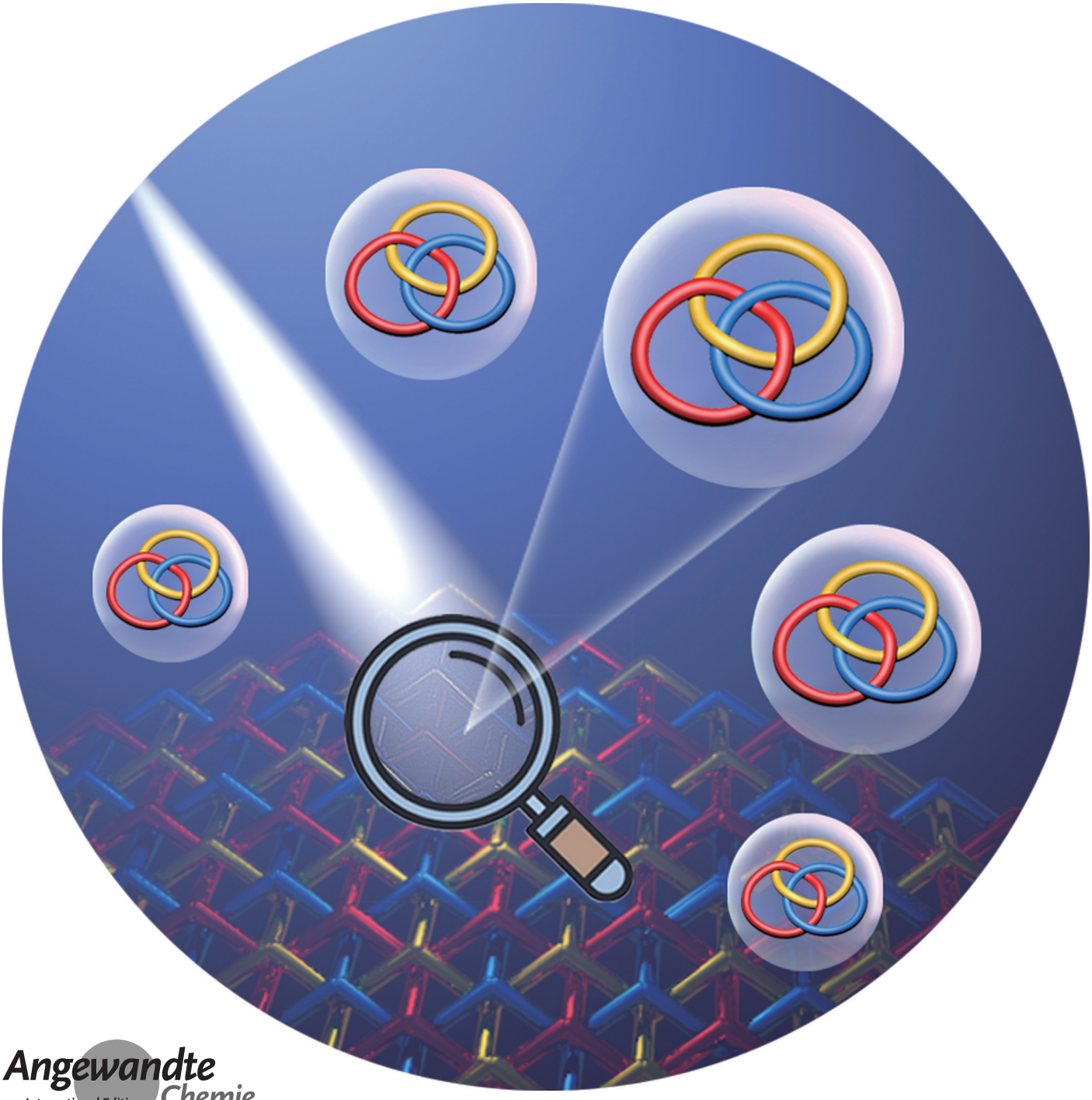

Abstract: *Attributed to the unique topological complexity and elegant beauty, Borromean systems are attracting intense attention. However, at present, the construction of Borromean linked organic polymers remains a challenge. To address this formidable challenge, we developed a supramolecular-synthon-driven approach to fabricate Borromean linked organic polymer. The solvothermal condensation reaction of a judiciously selected trigonal pyramidal building block, 1,3,5-Tris(4-aminophenyl)adamantane, with linear dialdehyde building blocks allowed the construction of two rare covalent organic frameworks (COFs) with high crystallinity and robustness. Structure refinement unveiled the successful formation of entangled 2D→2D Borromean arrayed structures. Both the two COFs were of microporosity and thus demonstrated the potentials for gas separation. The successful synthesis of the first two Borromean linked organic polymers paves the avenue to expand the supramolecular-synthon-driven approach to other building blocks and topologies, and broadens the family and scope of COFs.*

Introduction

In the past three decades, crystalline porous materials (CPMs)[1,2] including metal-organic frameworks (MOFs),[3,4] covalent organic frameworks (COFs),[5–9] hydrogen-bonded organic frameworks (HOFs),[10] zeolites,[11] metal-organic polyhedra (MOPs),[12,13] and porous organic cage (POC),[14] have achieved terrific progress in many research fields such as catalysis,[15] gas storage and separation,[16] electrochemistry,[17] drug delivery,[18] sensing[19] and fluorescence imaging,[20] attributed to their high crystallinity and regular porous structures. The outstanding properties of CPMs depend on their structures. However, the design, prediction, and rationalization of CPMs' structures are always of great challenge. Thanks to the pioneering works by Robson,[21] Yaghi,[22] O'Keeffe,[23] et al.,[24] the design and construction of desired CPM structures may be realized using the "node and linker" approach, and the reticular chemistry synthesis approach. However, obtaining the desired CPM structures is not always guaranteed.[25]

The Borromean links, in which three rings are interlocked and no two are interlinked, constitute topologically intriguing entanglement.[26] Attributed to their unique topological complexity, structural integrity, and elegant beauty, the Borromean systems have attracted the attention of scientists from various backgrounds.[27–29] The earliest example of molecular Borromean rings was reported in 1997 via manipulating DNA sequences.[30,31] In 2004, Stoddart and collaborators reported the first molecular Borromean links achieved by a coordination-driven assembly strategy.[32] Since Stoddart's pioneering work, coordination chemistry has been frequently used to drive the formation of Borromean arrayed structures. For example, Lu group synthesized a 2D→2D entangled coordination polymer with a Borromean structure.[33] Besides, Zheng and co-workers first reported the rational construction of HOFs with Borromean 3-fold 2D→2D entangled layers, and n-Borromean 2D→3D entangled infinite layers based on hydrogen-bond-driven self-assembly of 1,3,5-tris(4-carboxyphenyl)adamantane (TCA).[34] Overall, the development of Borromean systems is still underexplored, and creating advanced materials with desired Borromean structures is urgently demanded.

Since the pioneering work by Yaghi in 2005,[35] COFs have emerged a new class of CPMs with periodic networks linked by covalent bonds. However, up to now, the construction of COFs with Borromean links remains a formidable challenge. In order to design and synthesize Borromean arrayed COFs, three factors are essential: i) the 6^3 honeycomb net with large enough hexagonal cavities, which ensure the accommodation for other two nets; ii) the chair conformation of the hexagonal rings; iii) appropriate interactions between the modules at each intersection that can control the direction of interpenetration.[36] Based on the above considerations, we first created a supramolecular-synthon-driven approach to construct COFs with Borromean links (Scheme 1a). According to the literature survey,[34,36] 1,3,5-triphenyl-adamantane is a perfect module to build Borromean structures because it can form an "up-down" dimeric supramolecular synthon stabilized by C–H···π interactions to direct the interweaving and the packing of structures (Scheme 1b). Thereupon, to demonstrate the proof of concept, we judiciously chose a rigid and trigonal pyramidal molecule, 1,3,5-Tris(4-aminophenyl)adamantane (TAA), as the main building blocks for the

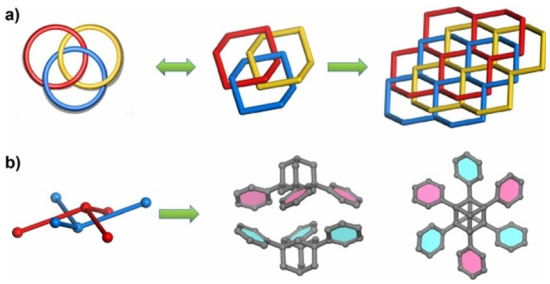

Scheme 1. a) The approach to build Borromean arrayed networks. b) The stable "up-down" dimeric supramolecular synthon formed by 1,3,5,-triphenyl-adamantane moieties.

[*] X. Guo,[+] E. Lin,[+] J. Gao, T. Mao, D. Yan, Prof. P. Cheng, Prof. Y. Chen, Prof. Z. Zhang
State Key Laboratory of Medicine Chemistry Biology, College of Chemistry, Nankai University
Tianjin 300071 (China)
E-mail: zhangzhenjie@nankai.edu.cn
X. Guo,[+] E. Lin,[+] J. Gao, T. Mao, D. Yan, Prof. P. Cheng, Prof. Z. Zhang
Renewable Energy Conversion and Storage Center, College of Chemistry, Nankai University
Tianjin 300071 (China)
Prof. P. Cheng, Prof. Z. Zhang
Key Laboratory of Advanced Energy Materials Chemistry, Ministry of Education, Nankai University
Tianjin 300071 (China)
Prof. S. Ma
Department of Chemistry, University of North Texas
1508 W Mulberry St, Denton, TX 76201 (USA)
[+] These authors contributed equally to this work.
Supporting information and the ORCID identification number(s) for the author(s) of this article can be found under: https://doi.org/10.1002/anie.202012504.

construction of Borromean linked COFs. Furthermore, linear linkers such as terephthalaldehyde (TP) and its extended variant (4,4′-biphenyldicarboxaldehyde, BPDA) were chosen as the guiding skeletons for the formation of two entangled 2D→2D Borromean layered structures, **NKCOF-6** and **-7** (NKCOF = Nankai University Covalent Organic Framework).

Results and Discussion

On this basis of the above design (Figure 1), the solvothermal reaction of TAA and TP in the mixed solvent of 1,2-dichlorobenzene, 1-butanol, and acetic acid at 120 °C for three days afforded a crystalline powder of **NKCOF-6** with a yield of ≈60 %. Subsequently, the as-prepared yellow powder was collected by filtration and washed by Soxhlet extraction. A variety of methods were employed for structural characterizations of **NKCOF-6**. The formation of **NKCOF-6** was assessed by the Fourier transform infrared (FT-IR) spectrum and ^{13}C cross-polarization magic-angle spinning (CP/MAS) NMR spectroscopy. Compared with the corresponding TAA and aldehydes monomer, the FT-IR spectrum revealed a new peak at 1621 cm^{-1} for **NKCOF-6** (Figure 2a), which is a typical characteristic of the C=N stretching vibrations. Meanwhile, the disappearance of the C=O stretching vibrations (1682 cm^{-1} for TP) and the N-H stretching vibrations (3441 cm^{-1} and 3363 cm^{-1} for TAA) indicated the complete transformation of aldehyde- and amine-containing reactants. The ^{13}C NMR spectroscopy further confirmed the successful formation of imine groups by the peak at 158.3 ppm for **NKCOF-6** (Figure 2b). Scanning electron microscopy (SEM) images revealed that **NKCOF-6** exhibited a distinctive homogeneous spheric morphology with approximately 2.1 μm diameter particles (Figure 2c). In addition, the successful synthesis of **NKCOF-6** was verified by the synthesis of a model compound by a reaction of TAA with benzaldehyde (Figure S1 and S2).

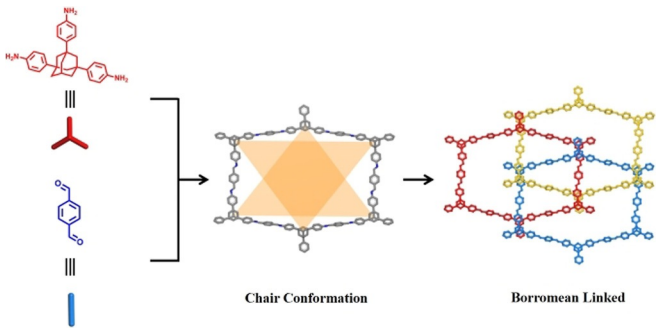

Figure 1. The synthetic route of **NKCOF-6**.

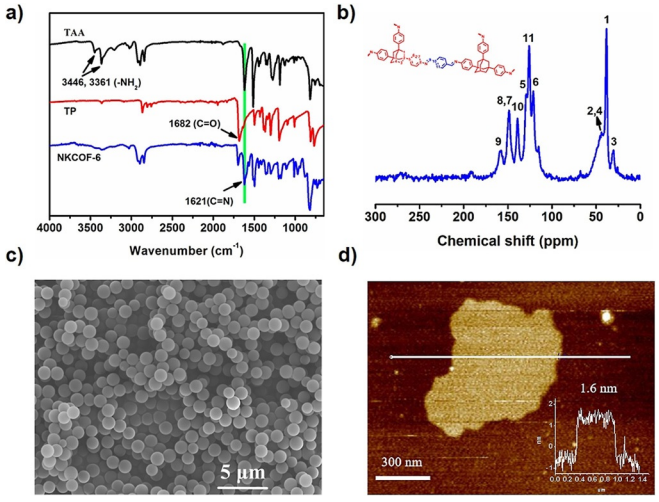

Figure 2. a) FT-IR spectra of **NKCOF-6** and corresponding monomers. b) ^{13}C CP/MAS solid-state NMR spectra of **NKCOF-6**. c) SEM image of **NKCOF-6**. d) AFM image and the height profile of **NKCOF-6**.

The as-prepared **NKCOF-6** was then submitted to the powder X-ray diffraction (PXRD) analysis to determine its crystal structure by comparing the experimental PXRD pattern with the theoretically simulated model,[37,38] which was conducted with the Materials Studio Software package. As shown in Figure 3, the two most intense diffraction peaks in the PXRD profile of **NKCOF-6** appeared at 4.26° and 5.82° (2θ). They exhibited strong diffraction intensity together with narrow Full width at half maximum (FWHM), indicating a high crystallinity of **NKCOF-6**. To solve the structure of **NKCOF-6**, we referred to the real crystal structures of Borromean linked HOFs reported by Zheng and co-workers. In these HOFs, the TCA dimers inside layered Borromean weaves were hydrogen-bonded with each other through -COOH groups in TCA. The hydrogen bonds between carboxylic acid dimer synthon were linear and coplanar. Therefore, these HOF structures can be treated as perfect models to solve the structure of **NKCOF-6**, via replacing the carboxylic acid dimer synthon by linear linkers such as p-phenyl diimine moieties (Figure S3). Based on this concept, we assumed the possible crystal structure of **NKCOF-6** was assembled with paralleled 2D honeycomb sheets, i.e., 3-fold interwoven structures with entangled ABC stacking analogous to the layered Borromean weaves. In the ideal case, TAA is considered as a C_3-symmetry molecule that possesses identical tetrahedral angles without distortion. However, in the real CPM networks, the tetrahedral angles are always distorted that break the intrinsic symmetry of TAA, hence leading to desymmetrize the network and lattice. This kind of

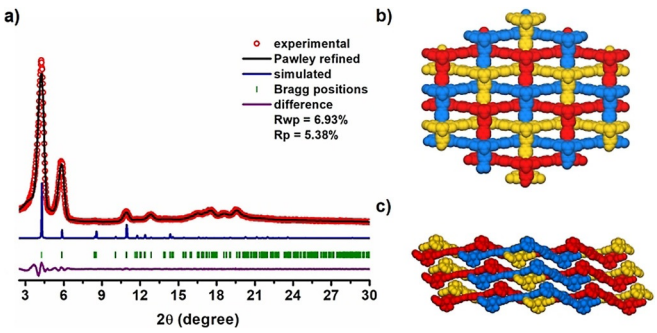

Figure 3. a) PXRD patterns of **NKCOF-6**. b) Space-filling model of Borromean weaves of **NKCOF-6**. Paralleled honeycomb sheets in layered Borromean weaves are shown as red, blue, gold. c) Separable Borromean weaves in **NKCOF-6**.

phenomenon has been observed in the HOFs reported by Zheng and co-workers.[31] Based on this hypothesis, we discovered a set of unit cell parameters ($a=b=22.5$ Å, $c=9.0$ Å, $\alpha=\beta=100°$, $\gamma=133°$) that matched the experimental PXRD pattern from both the positions and the intensities very well. All the observed diffraction peaks at d-spacing (2θ) 20.61 Å (4.27°), 15.15 Å (5.81°), 8.07 Å (10.90°), 6.85 Å (12.85°), 5.30 Å (16.6°), 5.00 Å (17.6°), can be assigned to (1 0 0), (1 −1 0), (0 1 −1), (3 0 0), (1 −3 0), and (3 −3 0) facets, respectively. Pawley refinement gave the unit-cell parameters of $a=22.6$ Å, $b=16.2$ Å, $c=9.0$ Å, $\alpha=94.2°$, $\beta=100.3°$ and $\gamma=110.6°$, with $R_{wp}=6.93\%$ and $R_p=5.38\%$. In the layer stacking model of **NKCOF-6** frameworks, adjacent adamantane vertices demonstrated a small ateral offset between adjacent COF layers (Figure 3c).

The structures of CPMs are categorized based on their underlying topologies, which can be described based on the number of vertices, edges, rings, and tiles. At present, the vast majority of reported COFs possess topologies with only one or two kinds of vertices and one kind of edge. For instance, the entangled ABC stacking models proposed above can be considered as the derivates of **dia-*z*** topology, with one kind of vertices and edges. Paralleled 2D honeycomb sheets with other stacking modes such as eclipsed AA stacking and AB stacking without entanglement, were also constructed as comparisons. However, both of them demonstrated a largely deviate from the experimental PXRD patterns (Figure S4). To further verify the correctness of Borromean linked ABC stacking model, we screened all the possible topologies that have one or two kinds of 3-connected vertices in the Reticular Chemistry Structure Resource (RCSR)[39] database. Totally, 193 topologies were identified and screened, and only two of them (**srs-c8**, **ths-c3**) were promising, in terms of their diffraction peak positions and relative intensity (Figure S4). However, these two networks depict much lower densities (**srs-c8**: 0.252 g cm^{-3}, **ths-c3**: 0.114 g cm^{-3}) than the experimental density (0.681 g cm^{-3}) measured for **NKCOF-6**. By contrast, the experimental density of **NKCOF-6** matched well with that of the Borromean layered structure (0.618 g cm^{-3}). The transmission electron microscopy (TEM) analyses revealed that **NKCOF-6** can be exfoliated into 2D nanosheets, consistent with the simulated layered structure (Figure S5). Atomic force microscopy (AFM) experiments were carried out to measure the thickness of the exfoliated nanosheets of **NKCOF-6** (Figure 2d and S6). The thickness of the thinnest nanosheet was measured to be about 1.6 nm, which was close to the monolayer thickness of proposed structure (1.4 nm). This result indicated that **NKCOF-6** possessed the predicted 2D layered structure.

To explore the generality of the supramolecular-synthon-driven approach to construct COFs with Borromean moieties, we used an extended variant of TP, i.e., BPDA, as the linear linker. The solvothermal reaction of TAA and BPDA afforded a pale yellow powder of **NKCOF-7** with a high yield of ≈83%. FI-IR spectra and solid-phase ^{13}C NMR further confirmed the existence of imine linkages in **NKCOF-7** (Figure S7 and S8). SEM analyses showed **NKCOF-7** exhibited a homogeneous spheric morphology with ≈1.3 μm particle size (Figure S9). Similar to **NKCOF-6**, the crystal

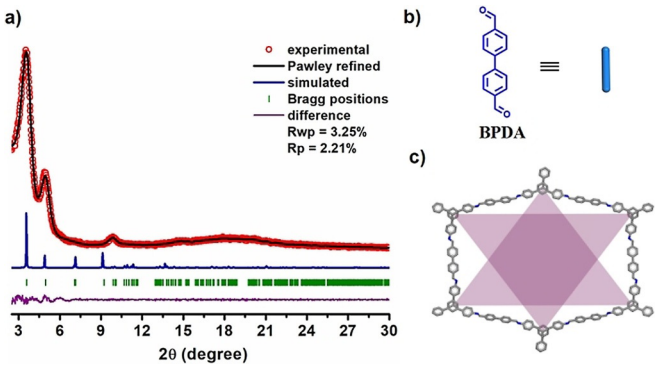

Figure 4. a) PXRD patterns of **NKCOF-7**. b) The linear linker of **NKCOF-7**. c) The hexagonal rings with chair conformation of **NKCOF-7**.

structure of **NKCOF-7** was also elucidated by comparing the experimental PXRD with the theoretically simulated ones. A series of peaks at d-spacing (2θ) 24.7 Å (3.56°), 18.0 Å (4.89°), and 8.97 Å (9.81°) are observed for **NKCOF-7** (Figure 4). We noted that the d-spacing of **NKCOF-7** diffraction peaks present equal proportion compared with that of **NKCOF-6**, and the scale factor is 1.1 approximately, which meant that **NKCOF-7** shared the identical structural feature with **NKCOF-6** and adapted the same stacking mode. The refined PXRD profile matched the experimental pattern quite well, giving unit cell parameters of $a=27.1$ Å, $b=19.3$ Å, $c=9.0$ Å, $\alpha=88.7°$, $\beta=81.2°$ and $\gamma=110.6°$, with $R_{wp}=3.25\%$ and $R_p=2.21\%$, respectively. In addition, the successful synthesis of **NKCOF-7** was verified by the synthesis of a model compound by a reaction of TAA with 4-Phenylbenzaldehyde (Figure S10 and S11).

The entangled Borromean networks usually exhibit higher stability than the structures without entanglement. NKCOFs was activated under vacuum at 120°C for 12 h before characterization. Thermal gravimetric analysis (TGA) measurement revealed **NKCOF-6** and **-7** could be thermally stable up to 450°C under N_2 without weight loss (Figure S12 and S13). The decomposition temperature is higher than some traditional imine-based COFs without entanglement (Table S3).[40–47] In addition, **NKCOF-6** and **-7** exhibited excellent chemical stability in various solvents, such as water, tetrahydrofuran (THF), N,N-dimethylformamide (DMF), acetone, acetonitrile and methanol (MeOH). Moreover, **NKCOF-6** and **-7** also exhibited good chemical stability under harsh conditions such as aqueous NaOH (1 M) and HCl (pH 2). PXRD data revealed that **NKCOF-6** and **-7** retained their crystalline structures after treatments under these conditions (Figure S14 and S15). The static water contact angle of the surface was measured to investigate the hydrophilic-hydrophobic property of COFs, that revealed a static water contact angles 95° for **NKCOF-6** and 101° for **NKCOF-7** (Figure S16). According to literature,[48] the hydrophobic property of NKCOFs could contribute to their high water stability.

The porosity and specific surface areas of **NKCOF-6** and **-7** were characterized by N_2 adsorption-desorption at 77 K (Figure 5). The adsorption isotherms of NKCOFs showed a sharp uptake at a low-pressure of P/P_0 range ($P/P_0=0$-0.05),

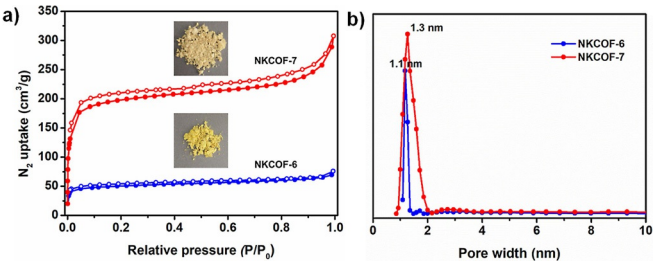

Figure 5. a) N_2 adsorption-desorption isotherms of **NKCOF-6** and **NKCOF-7** collected at 77 K. b) Pore size distributions of **NKCOF-6** and **NKCOF-7**.

which was a typical characteristic of microporous materials exhibited a classic type I isotherm. The Langmuir surface area of **NKCOF-6** and **-7** was calculated to be 328 $m^2 g^{-1}$ and 1052 $m^2 g^{-1}$, respectively. Pore size distributions calculated based on the nonlocal density functional theory (NLDFT) demonstrated an average pore size of 1.1 nm and 1.3 nm for **NKCOF-6** and **-7**, respectively, which are close to the values obtained from the Materials Studio and Poreblazer softwares.[49]

Given the microporous nature of **NKCOF-6** and **-7**, we investigated their potential application for gas separation. Currently, one of the urgent challenges in acetylene (C_2H_2) production is the removal of the co-existence of carbon dioxide (CO_2) impurities.[50] However, separation of C_2H_2 and CO_2 is of the paramount challenge because they possess very similar molecule shapes/sizes ($3.32 \times 3.34 \times 5.70$ Å^3 for C_2H_2 and $3.18 \times 3.33 \times 5.36$ Å^3 for CO_2), and similar physical properties (boiling points of 189.3 K and 194.7 K, respectively).[51] To address this challenge, we collected the single-component gas adsorption isotherms for C_2H_2 and CO_2 at 273 K and 298 K at 1 bar, respectively. As shown in Figure S17 and S18, the uptakes of **NKCOF-6** at 1 bar and 298 K were up to 30.9 $cm^3 g^{-1}$ and 15.6 $cm^3 g^{-1}$ for C_2H_2 and CO_2, respectively, which were higher than those of **NKCOF-7** (30.2 $cm^3 g^{-1}$ for C_2H_2, 13.8 $cm^3 g^{-1}$ for CO_2). The isosteric enthalpy (Q_{st}) can quantitatively evaluate the affinity of adsorbent toward adsorbate. Thus, we calculated the Q_{st} from the adsorption isotherms at 273 K and 298 K (Figure S19–S21). The initial Q_{st} are 27.1 kJ mol^{-1} and 25.1 kJ mol^{-1} of **NKCOF-6** for C_2H_2 and CO_2, respectively. The initial Q_{st} are 25.6 kJ mol^{-1} and 20.4 kJ mol^{-1} of **NKCOF-7** for C_2H_2 and CO_2, respectively. The higher Q_{st} of **NKCOF-6** agreed with the literature results that narrower pores usually led to stronger interaction for gas molecules.[52] Because the uptake and binding energy for C_2H_2 are larger than those for CO_2, NKCOFs have the potential for C_2H_2/CO_2 separation. To further examine this potential, we calculated C_2H_2/CO_2 selectivity (2:1) at 298 K and 1 bar using the ideal adsorption solution theory (IAST) (Figure S22).[53] The results revealed that **NKCOF-6** showed a higher C_2H_2/CO_2 selectivity than that for **NKCOF-7**. Breakthrough experiments for C_2H_2/CO_2 (2:1) at 298 K were also performed to evaluate the gas separation performance of these COFs (Figure S22). As expected, breakthrough experiments revealed that CO_2 was firstly eluted through the packed column, while C_2H_2 was still kept. Notably, the separation performance of **NKCOF-6** was better than that of **NKCOF-7**, consistent with the trend of the IAST result. To the best of our knowledge, we demonstrated the first two COFs, which achieved the real C_2H_2/CO_2 gas mixture separation in the COF field.[16]

Conclusion

In summary, we, for the first time, developed an efficient and versatile supramolecular-synthon-driven approach to construct COFs with Borromean links, which have not been achieved yet in the literature. A solvothermal condensation reaction of a judiciously selected trigonal pyramidal building block (1,3,5-Tris(4-aminophenyl)adamantane) with the linear terephthalaldehyde building block allowed the construction of a rare 2D imine-based COF (**NKCOF-6**) with high crystallinity and robustness. In order to determine the COF structure, we developed a novel strategy: using the real single-crystal structure of reported HOFs as the structure model and substituting the planar carboxylic acid dimer synthon in HOFs by p-phenyl diimine linear linker in COFs. Structure refinement unveiled that this COF possessed a twisted hexagonal crystal lattice and entangled 2D→2D Borromean layered structure. Furthermore, we proved the generality of the supramolecular-synthon-driven approach and successfully fabricated another Borromean linked COF, **NKCOF-7**, via extending the length of the dialdehyde linker. Moreover, both the two COFs were of microporosity and thus can be used to separate C_2H_2 over CO_2. This work not only enriched the family and scope of COFs, but also realized a new powerful strategy to fabricate Borromean linked materials.

Acknowledgements

The authors acknowledge the National Natural Science Foundation of China (21971126) and 111 Project (B12015). We also thank Dr. Kai Zhang and Haixia Li from Nankai University for the assistance of TEM and AFM tests.

Conflict of interest

The authors declare no conflict of interest.

Keywords: Borromean rings · covalent organic frameworks · entanglement · microporous structures · rational design

[1] J. Zhou, B. Wang, *Chem. Soc. Rev.* **2017**, *46*, 6927–6945.
[2] J. Jiao, W. Gong, X. Wu, S. Yang, Y. Cui, *Coord. Chem. Rev.* **2019**, *385*, 174–190.
[3] T. R. Cook, Y. R. Zheng, P. J. Stang, *Chem. Rev.* **2013**, *113*, 734–777.
[4] M. Bosch, S. Yuan, W. Rutledge, H. C. Zhou, *Acc. Chem. Res.* **2017**, *50*, 857–865.
[5] K. Geng, T. He, R. Liu, S. Dalapati, K. T. Tan, Z. Li, S. Tao, Y. Gong, Q. Jiang, D. Jiang, *Chem. Rev.* **2020**, *120*, 8814–8933.
[6] M. S. Lohse, T. Bein, *Adv. Funct. Mater.* **2018**, *28*, 1705553.
[7] S.-Y. Ding, W. Wang, *Chem. Soc. Rev.* **2013**, *42*, 548–568.

[8] Y. Jin, Y. Hu, W. Zhang, *Nat. Rev. Chem.* **2017**, *1*, 0056.
[9] X. Guan, F. Chen, Q. Fang, S. Qiu, *Chem. Soc. Rev.* **2020**, *49*, 1357 – 1384.
[10] R.-B. Lin, Y. He, P. Li, H. Wang, W. Zhou, B. Chen, *Chem. Soc. Rev.* **2019**, *48*, 1362 – 1389.
[11] C. S. Cundy, P. A. Cox, *Chem. Rev.* **2003**, *103*, 663 – 702.
[12] D. J. Tranchemontagne, Z. Ni, M. O'Keeffe, O. M. Yaghi, *Angew. Chem. Int. Ed.* **2008**, *47*, 5136 – 5147; *Angew. Chem.* **2008**, *120*, 5214 – 5225.
[13] E. J. Gosselin, C. A. Rowland, E. D. Bloch, *Chem. Rev.* **2020**, *120*, 8987 – 9014.
[14] T. Hasell, A. I. Cooper, *Nat. Rev. Mater.* **2016**, *1*, 16053.
[15] Y.-B. Huang, J. Liang, X.-S. Wang, R. Cao, *Chem. Soc. Rev.* **2017**, *46*, 126 – 157.
[16] Z. Wang, S. Zhang, Y. Chen, Z. Zhang, S. Ma, *Chem. Soc. Rev.* **2020**, *49*, 708 – 735.
[17] J. Li, X. Jing, Q. Li, S. Li, X. Gao, X. Feng, B. Wang, *Chem. Soc. Rev.* **2020**, *49*, 3565 – 3604.
[18] V. S. Vyas, M. Vishwakarma, I. Moudrakovski, F. Haase, G. Savasci, C. Ochsenfeld, J. P. Spatz, B. V. Lotsch, *Adv. Mater.* **2016**, *28*, 8749 – 8754.
[19] X. Liu, D. Huang, C. Lai, G. Zeng, L. Qin, H. Wang, H. Yi, B. Li, S. Liu, M. Zhang, R. Deng, Y. Fu, L. Li, W. Xue, S. Chen, *Chem. Soc. Rev.* **2019**, *48*, 5266 – 5302.
[20] L. He, T. Wang, J. An, X. Li, L. Zhang, L. Li, G. Li, X. Wu, Z. Su, C. Wang, *CrystEngComm* **2014**, *16*, 3259 – 3263.
[21] R. W. Gable, B. F. Hoskins, R. Robson, *J. Chem. Soc. Chem. Commun.* **1990**, 1677 – 1678.
[22] H. Li, M. Eddaoudi, M. O'Keeffe, O. M. Yaghi, *Nature* **1999**, *402*, 276 – 279.
[23] O. M. Yaghi, M. O'Keeffe, N. W. Ockwig, H. K. Chae, M. Eddaoudi, J. Kim, *Nature* **2003**, *423*, 705 – 714.
[24] X. Cui, K. Chen, H. Xing, Q. Yang, R. Krishna, Z. Bao, H. Wu, W. Zhou, X. Dong, Y. Han, B. Li, Q. Ren, M. J. Zaworotko, B. Chen, *Science* **2016**, *353*, 141.
[25] G. R. Desiraju, *Angew. Chem. Int. Ed.* **2007**, *46*, 8342 – 8356; *Angew. Chem.* **2007**, *119*, 8492 – 8508.
[26] L. Carlucci, G. Ciani, D. M. Proserpio, *Coord. Chem. Rev.* **2003**, *246*, 247 – 289.
[27] Y. Wang, J. F. Stoddart, *Chem* **2017**, *3*, 17 – 18.
[28] Y. Lu, Y.-X. Deng, Y.-J. Lin, Y.-F. Han, L.-H. Weng, Z.-H. Li, G.-X. Jin, *Chem* **2017**, *3*, 110 – 121.
[29] A. P. O. Chan, P. Ye, S. Ryu, *Phys. Rev. Lett.* **2018**, *121*, 061601.
[30] C. Mao, W. Sun, N. C. Seeman, *Nature* **1997**, *386*, 137 – 138.
[31] N. C. Seeman, *Acc. Chem. Res.* **1997**, *30*, 357 – 363.
[32] K. S. Chichak, S. J. Cantrill, A. R. Pease, S.-H. Chiu, G. W. V. Cave, J. L. Atwood, J. F. Stoddart, *Science* **2004**, *304*, 1308 – 1312.
[33] L. Jiang, X.-R. Meng, H. Xiang, P. Ju, D.-C. Zhong, T.-B. Lu, *Inorg. Chem.* **2012**, *51*, 1874 – 1880.
[34] Y.-B. Men, J. Sun, Z.-T. Huang, Q.-Y. Zheng, *Angew. Chem. Int. Ed.* **2009**, *48*, 2873 – 2876; *Angew. Chem.* **2009**, *121*, 2917 – 2920.
[35] A. P. Côté, A. I. Benin, N. W. Ockwig, M. Keeffe, A. J. Matzger, O. M. Yaghi, *Science* **2005**, *310*, 1166 – 1170.
[36] Y.-B. Men, J. Sun, Z.-T. Huang, Q.-Y. Zheng, *Chem. Commun.* **2010**, *46*, 6299 – 6301.
[37] C. Gao, J. Li, S. Yin, J. Sun, C. Wang, *J. Am. Chem. Soc.* **2020**, *142*, 3718 – 3723.
[38] T.-Y. Zhou, S.-Q. Xu, Q. Wen, Z.-F. Pang, X. Zhao, *J. Am. Chem. Soc.* **2014**, *136*, 15885 – 15888.
[39] M. O'Keeffe, M. A. Peskov, S. J. Ramsden, O. M. Yaghi, *Acc. Chem. Res.* **2008**, *41*, 1782 – 1789.
[40] P. J. Waller, S. J. Lyle, T. M. Osborn Popp, C. S. Diercks, J. A. Reimer, O. M. Yaghi, *J. Am. Chem. Soc.* **2016**, *138*, 15519 – 15522.
[41] Q. Sun, B. Aguila, J. A. Perman, T. Butts, F.-S. Xiao, S. Ma, *Chem* **2018**, *4*, 1726 – 1739.
[42] Y. Yang, X. He, P. Zhang, Y. H. Andaloussi, H. Zhang, Z. Jiang, Y. Chen, S. Ma, P. Cheng, Z. Zhang, *Angew. Chem. Int. Ed.* **2020**, *59*, 3678 – 3684; *Angew. Chem.* **2020**, *132*, 3707 – 3713.
[43] Y. Yusran, H. Li, X. Guan, D. Li, L. Tang, M. Xue, Z. Zhuang, Y. Yan, V. Valtchev, S. Qiu, Q. Fang, *Adv. Mater.* **2020**, *32*, 1907289.
[44] F. J. Uribe-Romo, C. J. Doonan, H. Furukawa, K. Oisaki, O. M. Yaghi, *J. Am. Chem. Soc.* **2011**, *133*, 11478 – 11481.
[45] H.-C. Ma, G.-J. Chen, F. Huang, Y.-B. Dong, *J. Am. Chem. Soc.* **2020**, *142*, 12574 – 12578.
[46] X. Han, Q. Xia, J. Huang, Y. Liu, C. Tan, Y. Cui, *J. Am. Chem. Soc.* **2017**, *139*, 8693 – 8697.
[47] S. Chandra, T. Kundu, S. Kandambeth, R. Babarao, Y. Marathe, S. M. Kunjir, R. Banerjee, *J. Am. Chem. Soc.* **2014**, *136*, 6570 – 6573.
[48] N. C. Burtch, H. Jasuja, K. S. Walton, *Chem. Rev.* **2014**, *114*, 10575 – 10612.
[49] L. Sarkisov, A. Harrison, *Mol. Simul.* **2011**, *37*, 1248 – 1257.
[50] R. Matsuda, R. Kitaura, S. Kitagawa, Y. Kubota, R. V. Belosludov, T. C. Kobayashi, H. Sakamoto, T. Chiba, M. Takata, Y. Kawazoe, Y. Mita, *Nature* **2005**, *436*, 238 – 241.
[51] C. R. Reid, K. M. Thomas, *J. Phys. Chem. B* **2001**, *105*, 10619 – 10629.
[52] R.-B. Lin, S. Xiang, W. Zhou, B. Chen, *Chem* **2020**, *6*, 337 – 363.
[53] D. DeSantis, J. A. Mason, B. James, J. R. Long, M. Veenstra, *Energy Fuels* **2017**, *31*, 2024 – 2032.

Manuscript received: September 14, 2020
Revised manuscript received: November 3, 2020
Accepted manuscript online: November 19, 2020
Version of record online: December 28, 2020

